THE JOURNAL OF PHYSICAL CHEMISTRY B

ARTICLE

pubs.acs.org/JPCB

Effect of High Pressure CO_2 on the Structure of PMMA: A FT-IR Study

Vito Di Noto,[*,†,‡] Keti Vezzù,[†,§] Guinevere A. Giffin,[†] Fosca Conti,[†] and Alberto Bertucco[∥]

[†]Department of Chemical Sciences, University of Padova, via Marzolo 1, I-35131 Padova, Italy

[‡]Institute of Molecular Science and Technology of the CNR of Padova, Via Marzolo 1, I-35131 Padova, Italy

[§]Department of Molecular Science and Nanosystems, University of Venezia, via Dorsoduro 2137, I-30123 Venezia, Italy

[∥]Department of Chemical Engineering, University of Padova, via Marzolo 9, 35131 Padova, Italy

ABSTRACT: Conformational changes in polymer films exposed to high-pressure CO_2 have been investigated with Fourier transform infrared (FT-IR) spectroscopy. The experimental setup, based on a custom-made stainless steel optical cell with CaF_2 windows, allows measurements in a CO_2 environment for pressures up to 6 MPa, in a temperature range from 293 to 353 K and in the mid-infrared (1000−4000 cm^{-1}). Poly(methyl methacrylate) (PMMA), a polymer with a side group (C-type), was studied to monitor the spectral changes as a function of CO_2 pressure and was compared to poly(D,L-lactic-*co*-glycolic acid) (PLGA), a polymer without a side group (B-type). By monitoring the characteristic carbonyl bands, conformational changes that occur due to molecular interactions between the high-pressure CO_2 and the polymers were explored at a constant pressurization rate (0.02 MPa/min) and temperature. Spectral changes are observed only for PMMA, where the vibrational band at 1680 cm^{-1} disappears with increasing pressure. The spectra of PLGA do not show any significant change in the presence of high pressure CO_2 in the investigated range. The behavior of the absorbance peak as a function of pressure and temperature highlights the presence of dynamic cross-links (DCs) between the side groups of PMMA films obtained by solvent casting below the glass transition temperature of the polymer. The spectral features are correlated using a model that accounts for CO_2 diffusion and the relaxation kinetics of the polymer chains in the thin film. The disappearance of the vibrational band attributed to the DCs for PMMA is related to the glass transition temperature, and a retrograde vitrification phenomenon is observed. This approach can be considered a useful alternative to magnetic suspended balance for the study of polymer−gas systems.

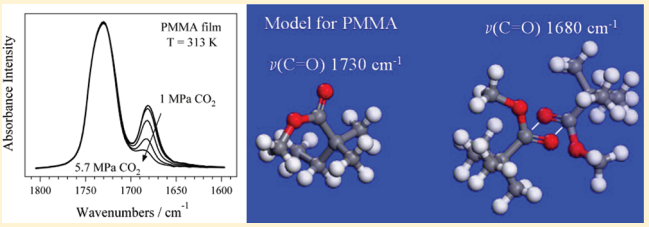

INTRODUCTION

Recently, significant attention has been focused on the potential applications of supercritical fluids in polymer processing, such as extrusion, foaming, micronization, impregnation, and reaction media,[1−5] because of the ability of supercritical fluids to modify the physical-chemical properties of polymers.[4,6−8] The compressed gases, which show liquid-like density and gas-like diffusivity, are quite soluble in polymers at moderate pressure, leading to depression of the melting and glass transition (T_g) temperatures and material swelling.[9−11] While these phenomena can lead to undesired effects such as the agglomeration of polymeric microparticles obtained by a supercritical anti-solvent process (SAS), they also can increase the efficiency of the impregnation process[12,13] or the yield of the polymer micronization by the particle from gas saturated solutions technique (PGSS).[14−16]

Carbon dioxide (CO_2) commonly is used as dense gas because it has a relatively low critical point (304 K, 7.4 MPa), is nontoxic, inexpensive, and has a minimal environmental impact. A number of studies about the effects of CO_2 on polymeric materials can be found in the literature. Wissinger et al.[17] focused their attention on the swelling effect of CO_2 on polymers. Handa et al.[18−21] studied the solubility, diffusivity, and plasticization effect of different polymers under high pressure gases such as methane, ethylene, and carbon dioxide. Kazarian et al.[22] described how the swelling of PMMA enhances the diffusion process in polymer dyeing by impregnation from a supercritical solution. Other recent works have examined the ability of CO_2 to plasticize polymers from a theoretical perspective. Condo et al.[9] described a model to predict the glass transition temperature of polymers in high-pressure gases based on a lattice-fluid state equation and the Gibbs−Di Marzio criterion. They also described a new phenomenon, called retrograde vitrification, which was experimentally demonstrated two years later.[23]

Despite several studies about macroscopic effects of high-pressure gases and supercritical fluids on polymers, there is a lack of molecular-level information on the interactions within the high-pressure gas−polymer systems. As a result, there exists a general perception that polymer swelling, gas sorption, and glass transition temperature depression are purely physical phenomena and not the result of specific chemical interactions between the gas/fluid and the polymer.

Recently, the interaction between CO_2 and carbonyl groups in low molecular weight molecules has been studied. Nelson et al.[24]

Received: August 17, 2011
Revised: October 13, 2011
Published: October 15, 2011

have suggested that the specific interaction between CO_2 and the carbonyl oxygen is a Lewis acid−base interaction, while Blatchford et al.[25] have suggested a cooperative intermolecular interaction between the oxygen of CO_2 and a hydrogen atom directly attached to the carbonyl group or in an α-position. Takahashi et al.[26] have examined the retrograde vitrification phenomena for the PMMA−CO_2 system with laser Raman spectroscopy and have developed a new method to derive the sorption kinetics of carbon dioxide.

Infrared spectroscopy is also an excellent tool to probe inter- and intramolecular interactions in polymer films subjected to high-pressure gases[27,28] and to study the heterogeneous catalyst in supercritical media.[2] Kazarian et al.[28−30] and, more recently, Shieh and Liu[31] have used the Fourier transform infrared (FT-IR) spectroscopy to investigate the interaction of carbon dioxide with polymers. They have shown that polymers possessing electron-donating functional groups (e.g., carbonyl groups) exhibit specific interactions with CO_2, which are likely of a Lewis acid−base nature. Surprisingly, Shieh and Liu[31] have found that the CO_2 was present in the PMMA film for about 6 months after the high pressure treatment.

FT-IR studies[22,30,32−37] have been used to probe the polymer−CO_2 interactions and polymer conformational changes. D'Illario et al.[38] examined the glass transition of poly(phenylene sulfide) by FT-IR at ambient pressure. The absorbance ratios of selected peaks as a function of the temperature showed an inflection point at the polymer glass transition temperature. Although relaxation phenomena of polymer chains occurring at the glass transition temperature are well characterized by calorimetric, dynamic-mechanical, and dielectric relaxation techniques, it is quite unusual to find FT-IR studies examining transition processes of pure polymers.[39,40]

In this work, structural changes related to the relaxation dynamics of the polymers, poly(methyl metacrylate) (PMMA) and poly(D,L-lactic-*co*-glycolic acid) (PLGA), under high-pressure CO_2 are investigated by FT-IR spectroscopy. PMMA was chosen because it is a standard polymer, widely used in the production of glass doors and acrylic varnishes. It is able to absorb a large amount of gas, which affects its properties such as the T_g.[8,9,23] PLGA is a biodegradable and biocompatible polymer which is widely used in the production of drug delivery systems by SAS techniques.[6,7,41−43] The study of plasticization of this amorphous polymer by CO_2 is strategically important because plasticization can result in unwanted microparticle agglomeration. However, when a solvent-free PGSS technique is employed, the plasticizing effect could result in successful polymer micronization.[6,13,15]

EXPERIMENTAL SECTION

Materials. CO_2 (99.998% purity) was supplied by Air Liquid (Padova, Italy); N_2 (99.999%), which was used for purging the apparatus before each experiment, was supplied by SIAD (Padova, Italy).

Poly(methyl methacrylate), PMMA (M_w = 101 kDa, T_g = 378 K), was purchased from Sigma (St. Louis, MO), and poly(D,L-lactic-*co*-glycolic acid), PLGA (M_w = 26 kDa, T_g = 317.61 K), was supplied by Alkermes (Cincinnati, OH).

Instrumentation and Sample Preparation. The FT-IR spectra were recorded using a Nicolet Nexus FT-IR spectrometer with a deuterated triglycine sulfate detector. A homemade stainless steel optical cell, with CaF_2 windows (Sigma-Aldrich, St Louis, MO) and a 10 mm path length, was used to collect spectra under high-pressure CO_2.[7] The 10 mm optical path length allows sufficient CO_2 to permit pressurization up to 12 MPa. The spectra are the result of averaging of 50 scans at a resolution of 4 cm^{-1}.

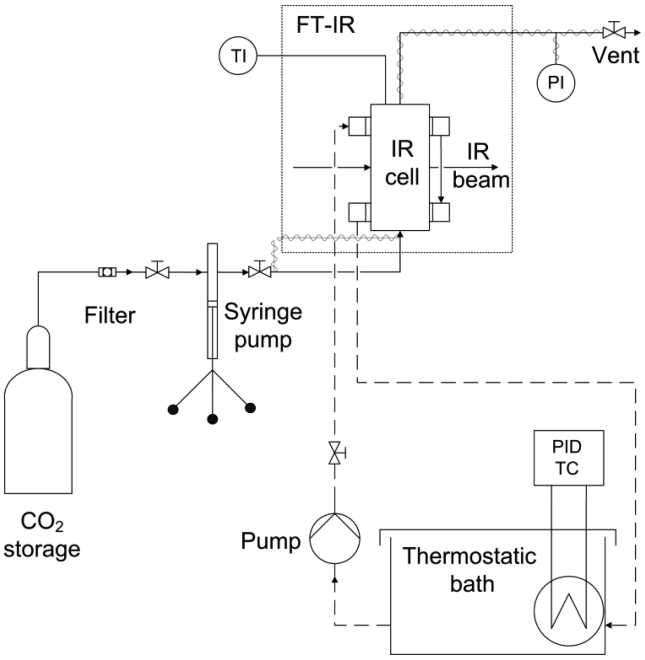

Figure 1. High-pressure FT-IR experimental apparatus. TI is the temperature indicator, PI is the pressure indicator, and PID TC is the PID temperature controller.

The polymer films were prepared by solvent casting the polymer solution directly onto CaF_2 windows. The window with the deposited polymer film was placed in an oven for 15 h at a temperature of ca. 313 K to completely remove the solvent. The PMMA solution was prepared by dissolving 2% (w/w) of the polymer in dichloromethane (DCM), while the PLGA solution was obtained by dissolving 5% (w/w) of the polymer in acetone. The thickness of both films was estimated with a micrometer to be 12 ± 2 μm. The windows were placed in the high pressure optical cell, and the entire system was purged with a N_2 flux at 0.1 MPa for 30 min at 20 cm^3/min flow rate. Finally, the cell was connected to the thermostatic bath and the high pressure CO_2 supply. Figure 1 shows the experimental setup employed. The N_2 was removed by purging the cell with CO_2 for 5 min at a high flow rate (100 cm^3/min) and low pressure (0.1 MPa). The experiments were performed at a constant pressurization rate, r, of 0.02 MPa/min, so the system is close to thermodynamic equilibrium.

Quantum Mechanical Calculations. First-principle calculations were carried out using density functional theory methods implemented in an all-electron DFT code using the DMol3 program[44,45] as a part of the Materials Studio package (double numerical plus polarization basis set, gradient-corrected (GGA) BLYP functional). The PMMA polymer was modeled using one repeat unit. The internal modes were identified by animating the atomic motion of each calculated mode using through features available in the DMol3 package.

RESULTS AND DISCUSSION

PMMA and PLGA are both polymers containing ester groups, but they are of different polymer classes. PMMA is a C-type

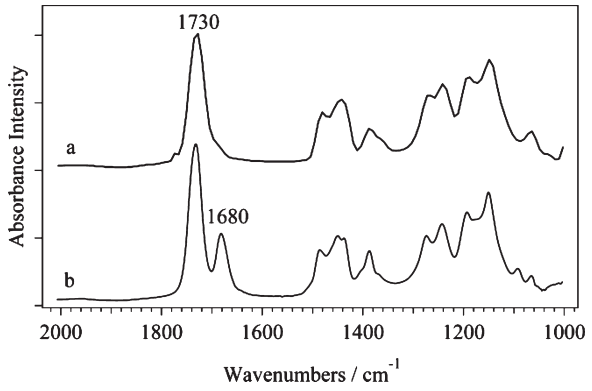

Figure 2. FT-IR spectra of PMMA: (a) powder as received and (b) film obtained by solvent casting from 2% (w/w) PMMA/DCM, both recorded at 298 K.

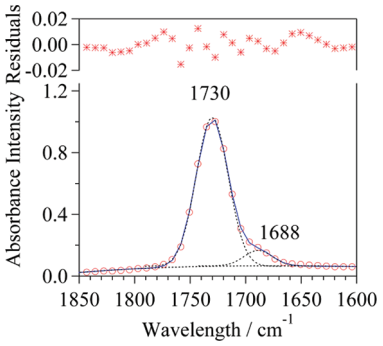

Figure 3. Decomposition of the carbonyl peak of PMMA powder (as received from Sigma). Circles, experimental data; solid line, fit curve; dashed lines, Gaussian peaks which result in the fit curve.

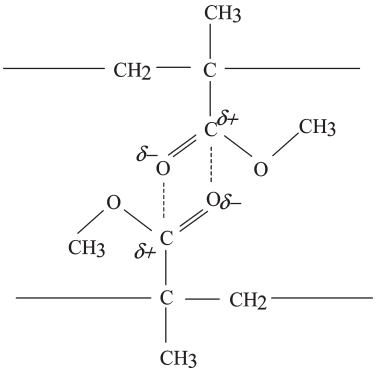

Figure 4. Possible dynamic cross-links (DCs) between PMMA side groups.

polymer, meaning that the polymer dipole is not located in the backbone but in the side chain. PLGA is a B-type polymer, where the polymer dipole is located in the main chain and is perpendicular to the polymer axis. This structural difference can have a significant impact on the organization of polymer chains.

The FT-IR spectra of the PLGA films do not show significant changes in the presence of CO_2 over the investigated temperature and spectral ranges of 283−353 K and 1000−4000 cm^{-1}, respectively, even at high pressure (6.0 MPa). Moreover, in applying the method proposed by D'Illario et al.,[38] the change in the absorbance ratios of selected peaks as a function of temperature and CO_2 pressure are found to be within experimental absorbance uncertainties. These results, when correlated to the PLGA structure, particularly the position of the carbonyl groups within the macromolecules, would indicate that the interaction of the high-pressure CO_2 with the polymer chain does not cause any substantial conformational changes. The absence of conformational changes has been observed despite the high CO_2 solubility in PLGA.[42,46] Additionally, no evidence of a glass transition can be found in the recorded spectra, which is detected by a variation in the slope of absorbance ratios of selected peaks plotted as a function of the pressure. The data are not shown in this work. For a detailed study on the interaction of CO_2 with PLGA, refer to the recent work of Tai et al.[47]

The FT-IR spectra of PMMA, which has a molecular structure characterized by ester side groups, are shown in Figure 2. The spectrum of the PMMA film shows a peak at 1680 cm^{-1}, on the low frequency side of the characteristic ester carbonyl mode at 1730 cm^{-1}. This lower frequency peak is also present as a shoulder in the as-received PMMA powder. This vibrational band has never been reported in the literature for PMMA. However, an examination of the published PMMA spectra reveals that this shoulder is clearly present in many of these spectra.[48−51] The intensity of the peak could be dependent on the molecular weight and the polydispersity. Decomposition of the as-received PMMA spectrum, as shown in Figure 3, shows that the carbonyl band is composed of two peaks: an intense peak centered at 1730 cm^{-1} and a weaker peak centered at 1688 cm^{-1} that is responsible for the low frequency shoulder.

The vibrational mode located between 1688 and 1680 cm^{-1} may be due to the CO stretching motion of interacting carbonyls. These interactions can occur between ester side groups belonging to either the same polymer chain (intramolecular/intrachain) or different polymer chains (intermolecular) and seems to be promoted by solvent casting from DCM. The interactions result in a link between side groups, dynamic cross-links (DCs), which could be considered the result of a dipolar-type interaction between the carbonyl groups. One possible geometry of the DCs is shown in Figure 4. Interaction of the carbonyl groups in such a geometry would result in a reduction of the force constant and, therefore, a reduction in the vibrational frequency of the carbonyl bond. It seems that this interaction is promoted in PMMA chains when the polymer is deposited via solvent casting from an organic solvent at temperatures below the glass transition temperature. These DCs are not highly stable. Both temperature and gas sorption can strongly influence the concentration of the DCs. A theoretical framework is proposed below to clarify these phenomena.

Quantum mechanical calculations are used to investigate the effect of interacting carbonyl groups on the characteristic C═O vibrational frequency. In an isolated methyl-capped monomer of PMMA, the frequency of the carbonyl stretching mode is 1709 cm^{-1}. This mode would correspond to the characteristic vibrational frequency of the carbonyl group, although it is calculated to be slightly lower in frequency than the band in Figure 2 at 1730 cm^{-1}. When two monomer units are arranged in the geometry shown in Figure 5, the vibrational motions of the carbonyl groups couple and both modes shift to lower frequencies. One mode at 1704 cm^{-1} results from an out-of-phase stretching motion involving both carbonyl units, while the other mode at 1698 cm^{-1} is due to in-phase coupling of these moieties. Both modes are at lower frequencies than that of the monomer. The distance between the carbonyl moieties in the calculated

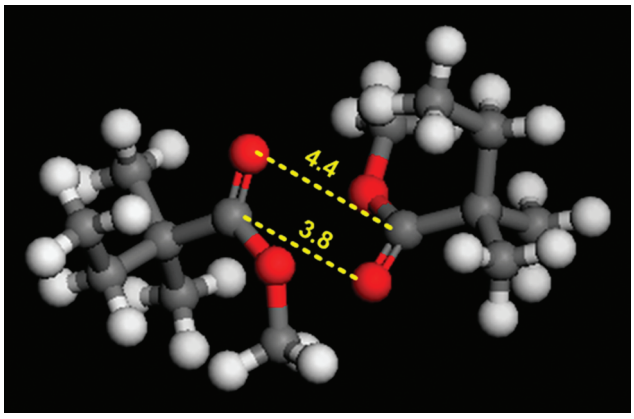

Figure 5. Optimized geometry used in the quantum chemical calculations of the vibrational frequencies for two interacting monomer units of PMMA.

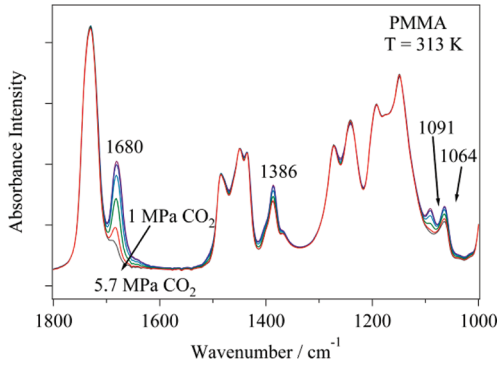

Figure 6. FT-IR spectra of PMMA film, obtained by solvent casting, recorded at 313 K as a function of CO_2 pressure (1, 2, 3, 4, 5, and 5.7 MPa). Spectra recorded at 1 and 2 MPa are indistinguishable. The peak observed at 1680 cm^{-1} is attributed to the presence of DCs.

geometry is approximately 3.8−4.4 Å. If this distance is reduced significantly, i.e., on the order of a carbonyl bond length, the interaction results in a dramatic reduction of the carbonyl frequency. In this scenario, the carbonyl mode has a frequency between 1050 and 900 cm^{-1}, which is characteristic of a C−O single bond. Additionally, this carbonyl mode is coupled with the C−O single bond present in the ester group. While such a small separation between carbonyl groups is highly unlikely in the solvent cast PMMA sample, this result demonstrates that an interaction between carbonyl units in the geometry shown in Figure 5 reduces the vibrational frequency. The band at 1680 cm^{-1} in Figure 2 is likely the superposition of the two calculated modes. There is also some evidence of asymmetry on the low frequency side of the 1680 cm^{-1} band, so it is possible that the two modes are not completely superimposed. The calculated results likely underestimate the strength of the interaction between the carbonyl groups. This would account for calculated frequencies that are higher than those found experimentally.

Figure 6 shows the change in the FT-IR profiles of PMMA over the spectral range of 1000−1800 cm^{-1} as the CO_2 pressure is increased from 1 to 5.7 MPa at 313 K. The spectra collected at 1 and 2 MPa are almost indistinguishable. However, as the CO_2 pressure rises, the intensity of the CO stretching mode at 1680 cm^{-1} decreases and disappears at pressures above 6 MPa.

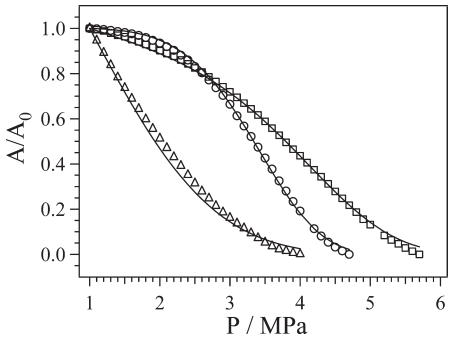

Figure 7. Absorbance profile corresponding to the vibrational band at 1680 cm^{-1} as a function of CO_2 pressure. The symbols represent the experimental data at three different temperatures: 303 K (circle), 333 K (square), and 353 K (triangle). The solid lines represent computer simulations following the theoretical model presented in the text.

In addition to the dramatic change in the peak at 1680 cm^{-1}, the intensity of the peaks at 1386, 1091, and 1064 cm^{-1} decreases. The peaks at 1091 and 1064 cm^{-1} are in the generally accepted range for a C−O stretching motion of esters containing $-OCH_3$ moieties.[52] The mode at 1091 cm^{-1} can be assigned to the C−O stretching motion of a side chain interacting in a geometry shown in Figure 5. The intensity of this band decreases along with the band at 1680 cm^{-1} and cannot be seen at high pressures. The intensity of the 1064 cm^{-1} band also decreases but not at the same rate as the peak at 1091 cm^{-1}. Given the close proximity of these bands, the total intensity of the 1064 cm^{-1} is affected by the rapidly decreasing intensity of the band at 1091 cm^{-1} that are likely partially overlapped.

The thermal dependence of the intensity of the 1680 cm^{-1} peak as a function of CO_2 pressure is shown in Figure 7. The rate of disappearance of this peak is strongly related to temperature. By increasing the pressure at 353 K (triangles in Figure 7), the intensity immediately decreases, whereas at 333 K (squares in Figure 7) the absorbance shows a gradual decrease at lower pressures and the rate of decrease increases with the pressure. At 303 K (circles in Figure 7), the peak intensity remains fairly constant until about 2 MPa where it starts to show a significant decrease. The complete disappearance of the 1680 cm^{-1} band occurs at a lower pressure in the 353 K isotherm than in either of the lower temperature isotherms because increased temperature increases the chain mobility[53] and disrupts the DCs. For the lower isotherms, the behavior is more complex. Increasing the pressure has the opposite effect of temperature, resulting in decreased chain mobility and increased gas sorption.[46,54] However, CO_2 has a plasticizing effect on PMMA,[4] so increasing the CO_2 pressure increases the chain mobility. The 303 K isotherm shows the disappearance of the 1680 cm^{-1} band at a lower pressure than the 333 K isotherm which indicates that at lower temperatures the plasticization of PMMA by CO_2 disrupts the DCs. However, the higher temperature isotherm (333 K) shows a higher initial rate of decrease. This implies that, at lower pressures, the temperature effect is dominant. Taken together, these results indicate that increasing the temperature at constant pressure will lead to a decreasing concentration of DCs if the effect of the temperature is strong enough to overcome decreased CO_2 sorption. It is well-known that PMMA absorbs CO_2,[17,20,46] which causes polymer swelling and increases the chain mobility.

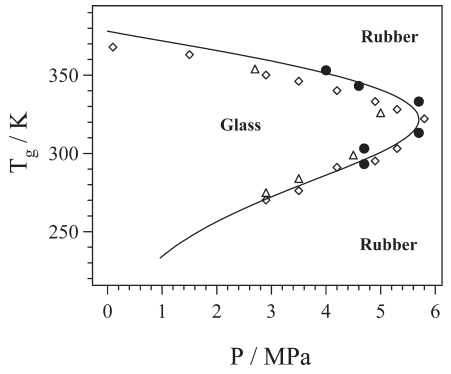

Figure 8. Dependence of the glass transition temperature, T_g, of the PMMA−CO_2 system on the CO_2 gas pressure. The solid line represents the solution of Condo's model and the retrograde vitrification phenomenon. ●, this work; △, ref 20; ◇, ref 54.

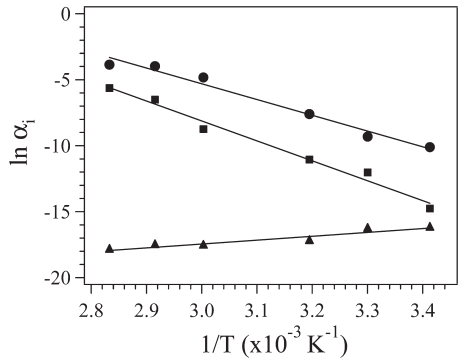

Figure 9. Temperature dependence of α_i (circles, $i = 0$; squares, $i = 1$; triangles, $i = 4$,). The solid lines represent the result of eq 12.

It is possible that the absorbed gas can interact with the DCs, causing the dissolution of these structures and, therefore, the disappearance of their characteristic peaks.

The values of temperature and pressure that correspond to the disappearance of the peak at 1680 cm^{-1} should be related to the mobility of the polymer side groups. This behavior can be related to the glass transition temperature (T_g) as defined by the Gibbs−Di Marzio criterion,[9,23] which states that the conformational entropy of a mixed system should go to zero at the glass transition.

Figure 8 reports the experimental values of temperature and pressure corresponding to the complete disappearance of the 1680 cm^{-1} vibrational band from the FT-IR spectra. The glass transition temperatures measured by Handa et al. using a stepwise temperature scanning high-pressure calorimetric technique and magnetic suspended balance[20,54] are also shown in Figure 8. There is good agreement between these sets of data.

The polymer−gas system exists as a glass within the T_g−P_g phase envelope and as a rubber outside this envelope. This type of glass transition behavior is known as retrograde vitrification.[9] The glass transition curve as a function of pressure is obtained by simultaneously solving the lattice-fluid equation of states and the Gibbs−Di Marzio criterion as proposed by Condo et al.[7] For this calculation, the approach suggested by Kikic et al.[55] is used to evaluate the pure component and interaction parameters of the state equation, the lattice coordination number, and the intramolecular flexing-bond entropy.

As the experimental interpretation of the glass transition temperature for PMMA is able to reproduce the complex phenomena of the retrograde vitrification, this methodology introduces a new approach to study the polymer−gas system.

A chemical kinetic model can be used to explain the disappearance of the 1680 cm^{-1} vibrational band due to the effect of temperature and high-pressure CO_2 sorption. Since the local concentration of CO_2 in the polymer affects the behavior of the polymer−gas system, it is useful to know the CO_2-concentration profile as a function of pressure and temperature for the thin polymer film.

A mass transfer model, based on Fick's law of diffusion, is employed to determine the characteristic CO_2 diffusion time (τ_D) as in eq 1.

$$\tau_D = L_s^2 / D_{CO_2\text{-PMMA}} \quad (1)$$

Here, L_s is the thickness of the polymer films and $D_{CO_2\text{-PMMA}}$ is Fick's diffusion coefficient for CO_2 in PMMA, which has been experimentally determined by Handa et al.[21] They have found that $D_{CO_2\text{-PMMA}}$ ranges from 1.2×10^{-9} to 1.2×10^{-7} cm^2/s over temperatures and pressure conditions from 300 K and 1.2 MPa to 355 K and 6.2 MPa.

On the basis of the lowest diffusion coefficient value, a characteristic diffusion time of around 10 min can be expected, which is small in comparison to the pressurization rate of 0.02 MPa/min. Using an average value for the diffusion coefficient (ca. 10^{-8} cm^2/s), the characteristic diffusion time decreases to 1 min. As a further check, the numerical solution of a time-dependent mass balance for CO_2 in equilibrium with the polymer film is considered. For a polymer film with a thickness of 15 μm under a pressurization rate of 0.02 MPa/min, an essentially constant CO_2 concentration profile is obtained. In a comparison of the CO_2 concentration at the interface and within the polymer films, a difference of only 5.7% is calculated for the lowest value of the diffusion coefficient.[7] Therefore, in the following theoretical model, it is safe to assume that the CO_2 concentration in the polymer film is at equilibrium.

The disappearance of the 1680 cm^{-1} characteristic peak is described using a chemical kinetic model based on parallel reactions that occur between the polymer side groups (PSGs) forming the DCs and CO_2.

$$\begin{cases} \text{PSGs} + \nu_0 CO_2 \leftrightarrow A_0^* \rightarrow d_0 \\ \text{PSGs} + \nu_1 CO_2 \leftrightarrow A_1^* \rightarrow d_1 \\ \quad\quad \cdots \\ \text{PSGs} + \nu_i CO_2 \leftrightarrow A_i^* \rightarrow d_i \end{cases} \quad (2)$$

In eq 2, ν_i is the molecularity of i, which refers to the number of CO_2 molecules involved in the interaction, and is unknown. A_i^* is an activated state in equilibrium with the reactants and d_i is the product of the reaction, i.e., the dissociated DC that is surrounded by ν_i CO_2 molecules. For $\nu_i = 0$, only the effect of the temperature must be considered.

The equilibrium constant (K_i) for a generic reaction i can be expressed by the ratio

$$K_i = \frac{[A_i^*]}{[CO_2]^{\nu_i}[\text{PSGs}]} \quad (3)$$

The concentration of CO_2 can be obtained from the literature[17] and for pressures lower than 6 MPa. $[CO_2]$ can be determined using an empirical equation that is a function of the pressure p of

the system

$$p = H_{CO_2}[CO_2] \quad (4)$$

where H_{CO_2} is an empirical constant typical for PMMA.

The concentration of the PGSs could be determined by the following mass balance

$$-\frac{\partial[PSG]}{\partial t} = \sum_i k_i[A_i^*] \quad (5)$$

where k_i is the rate of reaction i. Assuming a linear dependence of the pressure p on time, it is possible to write

$$-\frac{d[PSG]}{dp} = \sum_i \alpha_i p^{\nu_i}[PSG] \quad (6)$$

$$\alpha_i = rK_ik_i/H_{CO_2}^{\nu_i} \quad (7)$$

where α_i shown in eq 6 and defined in eq 7 is a parameter related to the pressurization rate. Finally, by integrating eq 5 and using the Lambert−Beer relation, the relative concentration of PGSs may be correlated to the absorbance of the 1680 cm^{-1} peak.

$$\frac{[PSG]}{[PSG]_0} = \frac{A}{A_0} = \prod_i \exp -\frac{\alpha_i(p^{\nu_i+1} - p_0^{\nu_i+1})}{\nu_i + 1} \quad (8)$$

In eq 8, A represents the absorbance and the subscript 0 refers to the initial conditions at p = 0.1 MPa.

Fitting the experimental data with eq 8 provides the values of the α_i parameters, which can be used to estimate the rate constant k_i of the process as in eq 9.

$$\ln \alpha_i = \ln \frac{rK_ik_i}{H_{CO_2}^{\nu_i}} \quad (9)$$

An Arrhenius-type equation can be considered for the temperature dependence of both the rate and equilibrium constants, k_i and K_i,

$$k_i = f_0 \exp\left(-\frac{E_a^k}{RT}\right) \quad (10)$$

$$K_i = F_0 \exp\left(-\frac{E_a^K}{RT}\right) \quad (11)$$

where f_0 and F_0 are pre-exponential factors and $E_a{}^k$ and $E_a{}^K$ are activation energies for the rate and equilibrium constants, respectively. R is the gas constant, and T is the absolute temperature. Using eqs 10 and 11, it is possible to rewrite eq 9.

$$\ln \alpha_i = m + \frac{n}{T} \quad (12)$$

m and n are constants expressed by eqs 13 and 14.

$$m = \ln F_0 + \ln f_0 - \ln rH_{CO_2}^{\nu_i} \quad (13)$$

$$n = -\frac{E_a^k + E_a^K}{R} \quad (14)$$

The experimental data were fitted with eq 8 using the least-squares method. Three different parallel reactions are considered in eq 8 to account for the temperature and CO_2 sorption contributions. The model is a product of three terms as in eq 15.

$$\frac{A}{A_0} = \exp[-\alpha_0(p - p_0)] \times \exp\left[-\alpha_1\frac{(p^2 - p_0{}^2)}{2}\right] \times \exp\left[-\alpha_4\frac{(p^5 - p_0{}^5)}{5}\right] \quad (15)$$

α_1 = 1 and α_4 = 4 account for CO_2 sorption, whereas α_0 = 0 considers only the temperature effect.

Only three terms were used in order to use the fewest possible fitting parameters that were needed to describe the most important physical events. It should be highlighted that there is little difference between i = 2, 3, and 4. The term α_i = 0 accounts for thermal effects in the absence of CO_2. The term α_i = 1 implies the presence of one CO_2 molecule that is largely responsible for the solvation of the PMMA side chain. The additional CO_2 molecules added in terms 2, 3, and 4 are bound with very rapid processes likely within a second solvation shell composed of CO_2 clusters. In order to minimize the number of fitting parameters involved, only α_i = 4 was used to model the formation of a high molecularity solvation cluster because the difference between the product of the terms containing α_i = 2, 3, and 4 and the term containing only α_i = 4 was negligible. This illustrates that the model is reasonable, as the data could be fit with three parameters as opposed to five. The results of eq 15 are shown as the solid line in Figure 7 and are reported for 303, 333, and 353 K. The model is able to accurately describe the experimental absorbance ratio profile and reproduces the experimental pressure corresponding to the disappearance of the 1680 cm^{-1} vibrational band.

The values of α_i, which are shown in Figure 9 for all isotherms (293, 303, 313, 333, 343, and 353 K), can be described by the linear function in eq 12. It is interesting to note that α_0 and α_1, which correspond to low CO_2 molecularity (ν_1 = 1 and ν_0 = 0), are dominant at higher temperatures, while α_4, which corresponds to a molecularity of ν_4 = 4, is essentially negligible. At low temperature when CO_2 sorption is favored, α_0 and α_1 are much lower and the contribution of α_4, which corresponds to a CO_2 solvation cluster, is no longer insignificant.

CONCLUSION

The innovative experimental setup, based on transmission FT-IR spectroscopy, developed in this work allows a rational understanding of the conformational changes that take place when a polymer thin film is exposed to high pressure CO_2. Spectral changes are observed only for PMMA, where the vibrational band at 1680 cm^{-1} disappears with increasing pressure. This band, although evident in previously published spectra, was not previously studied. The behavior of the absorbance peak, as a function of pressure and temperature, highlights the presence of dynamic cross-links between side groups of PMMA films obtained by solvent casting below the glass transition temperature of the polymer. The dissociation behavior of these DCs is complex due to the varying effects of temperature, gas pressure, and CO_2 plasticization on the chain mobility. The features of the PMMA spectra are correlated using a model that accounts for CO_2 diffusion and the relaxation kinetics of the polymer chains in the thin film. At lower temperatures where CO_2 sorption is favorable, the model supports a larger CO_2 molecularity for the dissociation reaction. However, at higher temperatures, the model indicates a lower molecularity of CO_2. Taken together,

the model suggests that plasticization by CO_2 is a significant factor in chain mobility at low temperatures, while the temperature effect on chain mobility is important at higher temperatures. The disappearance of the vibrational bands attributed to the DCs for PMMA can be related to the glass transition temperature. Such a correlation reveals a retrograde vitrification phenomenon, in agreement with previous works. This study demonstrates that temperature and pressure dependent FT-IR can be considered a useful alternative to magnetic suspended balance for the study of polymer−gas systems.

AUTHOR INFORMATION

Corresponding Author

*Phone/Fax: +39 049 8275229. E-mail: vito.dinoto@unipd.it.

ACKNOWLEDGMENT

The authors are grateful to Mr. L. Gelmi, Dr. Nicola Elvassore, and Eng. A. Favaro for assistance in equipment design. This work was financed by the Italian Ministry for the University and for Scientific and Technological Research (MURST) and by the University of Padova.

REFERENCES

(1) Cooper, A. I. *J. Mater. Chem.* **2000**, *10*, 207.
(2) Grunwaldt, J.-D.; Baiker, A. *Phys. Chem. Chem. Phys.* **2005**, *7*, 3526.
(3) Jung, J.; Perrut, M. *J. Supercrit. Fluids* **2001**, *20*, 179.
(4) Knez, Z.; Habulin, M. *J. Supercrit. Fluids* **2002**, *23*, 29.
(5) Tomasko, D. L.; Li, H.; Liu, D.; Han, X.; Wingert, M. J.; Lee, L. J.; Koelling, K. W. *Ind. Eng. Chem. Res.* **2003**, *42*, 6431.
(6) Di Noto, V.; Vezzù, K.; Pace, G.; Vittadello, M.; Bertucco, A. *Electrochim. Acta* **2005**, *50*, 3904.
(7) Striolo, A.; Favaro, A.; Elvassore, N.; Bertucco, A.; Di Noto, V. *J. Supercrit. Fluids* **2003**, *27*, 283.
(8) Vezzù, K.; Zago, V.; Vittadello, M.; Bertucco, A.; Di Noto, V. *Electrochim. Acta* **2006**, *51*, 1592.
(9) Condo, P. D.; Sanchez, I. C.; Panayiotou, C. G.; Johnston, K. P. *Macromolecules* **1992**, *25*, 6119.
(10) Wang, J.; Wang, M.; Hao, J.; Fujita, S.-i.; Arai, M.; Wu, Z.; Zhao, F. *J. Supercrit. Fluids* **2010**, *54*, 9.
(11) Yu, Y.; Yang, X. *Phys. Chem. Chem. Phys.* **2011**, *13*, 282.
(12) Sicardi, S.; Manna, L.; Banchero, M. *Ind. Eng. Chem. Res.* **2000**, *39*, 4707.
(13) Vezzù, K.; Betto, V.; Elvassore, N. *Biochem. Eng. J.* **2008**, *40*, 241.
(14) Knez, Z. Micronization of pharmaceuticals using supercritical fluids. In *Proceedings of the Seventh Meeting on Supercritical Fluids*; Perrut, M., Reverchon, E., Eds.; Antibes: France, 2000; Vol. *1*, p 21.
(15) Vezzù, K.; Borin, D.; Bertucco, A.; Bersani, S.; Salmaso, S.; Caliceti, P. *J. Supercrit. Fluids* **2010**, *54*, 328.
(16) Vezzù, K.; Campolmi, C.; Bertucco, A. *Int. J. Chem. Eng.* **2009**, Article ID 781247.
(17) Wissinger, R. G.; Paulaitis, M. E. *J. Polym. Sci., Part B: Polym. Phys.* **1987**, *25*, 2497.
(18) Handa, Y. P.; Kruus, P.; O'Neill, M. *J. Polym. Sci., Part B: Polym. Phys.* **1996**, *34*, 2635.
(19) Handa, Y. P.; Wong, B.; Zhang, Z.; Kumar, V.; Eddy, S.; Khemani, K. *Polym. Eng. Sci.* **1999**, *39*, 55.
(20) Handa, Y. P.; Zhang, Z. *Cell. Polym.* **2002**, *21*, 221.
(21) Handa, Y. P.; Zhang, Z.; Wong, B. *Cell. Polym.* **2001**, *20*, 1.
(22) Kazarian, S. G.; Brantley, N. H.; West, B. L.; Vincent, M. F.; Eckert, C. A. *Appl. Spectrosc.* **1997**, *51*, 491.
(23) Condo, P. D.; Johnston, K. P. *J. Polym. Sci., Part B: Polym. Phys.* **1994**, *32*, 523.
(24) Nelson, M. R.; Borkman, R. F. *J. Phys. Chem. A* **1998**, *102*, 7860.
(25) Blatchford, M. A.; Raveendran, P.; Wallen, S. L. *J. Phys. Chem. A* **2003**, *107*, 10311.
(26) Takahashi, M.; Yamamoto, Y.; Nawaby, A. V.; Handa, Y. P. *J. Polym. Sci., Part B: Polym. Phys.* **2003**, *41*, 2214.
(27) Howdle, S. M.; George, M. W.; Poliakoff, M. Spectroscopy of SCF Solutions. In *Chemical Synthesis Using Supercritical Fluids*; Jessop, P. G., Leitner, W., Eds.; Wiley-VCH: Weinheim, Germany, 1999; p 147.
(28) Kazarian, S. G.; Vincent, M. F.; Bright, F. V.; Liotta, C. L.; Eckert, C. A. *J. Am. Chem. Soc.* **1996**, *118*, 1729.
(29) Fleming, O. S.; Chan, K. L. A.; Kazarian, S. G. *Polymer* **2006**, *47*, 4649.
(30) Kazarian, S. G.; Chan, K. L. A. *Macromolecules* **2004**, *37*, 579.
(31) Shieh, Y.-T.; Liu, K.-H. *J. Supercrit. Fluids* **2003**, *25*, 261.
(32) Flichy, N. M. B.; Kazarian, S. G.; Lawrence, C. J.; Briscoe, B. J. *J. Polym. Sci., Part B: Polym. Phys.* **2001**, *39*, 3020.
(33) Flichy, N. M. B.; Kazarian, S. G.; Lawrence, C. J.; Briscoe, B. J. *J. Phys. Chem. B* **2002**, *106*, 754.
(34) Matsuyama, K.; Mishima, K. *J. Phys.: Conf. Ser.* **2010**, *215*, 012086.
(35) Vincent, M. F.; Kazarian, S. G.; Eckert, C. A. *Abstracts of Papers of the American Chemical Society*; American Chemical Society: Washington, DC, 1996; Vol. 211, pp PMSE.
(36) Vincent, M. F.; Kazarian, S. G.; Eckert, C. A. *AIChE J.* **1997**, *43*, 1838.
(37) Yokoyama, C.; Kanno, Y.-i.; Takahashi, M.; Ohtake, K.; Takahashi, S. *Rev. Sci. Instrum.* **1993**, *64*, 1369.
(38) D'Ilario, L.; Lucarini, M.; Martinelli, A.; Piozzi, A. *Eur. Polym. J.* **1997**, *33*, 1809.
(39) Koenig, J. L.; Antoon, M. K. *J. Polym. Sci., Part B: Polym. Phys.* **1977**, *15*, 1379.
(40) Magonov, S. N.; Shen, D.; Qian, R. *Makromol. Chem.* **1989**, *190*, 2563.
(41) Perrut, M. *STP Pharma Sci.* **2003**, *13*, 83.
(42) Sproule, T. L.; Lee, J. A.; Li, H.; Lannutti, J. J.; Tomasko, D. L. *J. Supercrit. Fluids* **2004**, *28*, 241.
(43) Vezzù, K.; Elvassore, N.; Bertucco, A.; Cecchi, A.; Caliceti, P. Protein Loading in Biodegradable Polymeric Microparticles Produced by Compressed Gas Antisolvent Technique. In *4th International Symposium on High Pressure Process Technology and Chemical Engineering*, Venice, Italy, 2002.
(44) Delley, B. *J. Chem. Phys.* **1990**, *92*, 508.
(45) Delley, B. *J. Chem. Phys.* **2000**, *113*, 7756.
(46) Elvassore, N.; Vezzù, K.; Bertucco, A. *J. Supercrit. Fluids* **2005**, *33*, 1.
(47) Tai, H.; Upton, C. E.; White, L. J.; Pini, R.; Storti, G.; Mazzotti, M.; Shakesheff, K. M.; Howdle, S. M. *Polymer* **2010**, *51*, 1425.
(48) Nagai, H.; Watanabe, H.; Nishioka, A. *J. Polym. Sci.* **1962**, *62*, S95.
(49) Schmidt, P.; Schneider, B.; Dirlikov, S.; Mihailov, M. *Eur. Polym. J.* **1975**, *11*, 229.
(50) Schneider, B.; Stokr, J.; Schmidt, P.; Mihailov, M.; Dirlikov, S.; Peeva, N. *Polymer* **1979**, *20*, 705.
(51) Stuart, B. *Modern Infrared Spectroscopy*; Wiley: Chichester, U.K., 1996.
(52) Lin-Vien, D.; Colthup, N. B.; Fateley, W. G.; Grasselli, J. G. *The Handbook of Infrared and Raman Characteristic Frequencies of Organic Molecules*; Academic Press, Inc.: New York, 1991.
(53) Strobl, G. R. *The Physics of Polymers: Concepts for Understanding their Structures and Behavior*, 2nd ed.; Springer: Heidelberg, Germany, 1997.
(54) Handa, Y. P.; Zhang, Z. *J. Polym. Sci., Part B: Polym. Phys.* **2000**, *38*, 716.
(55) Kikic, I.; Vecchione, F.; Alessi, P.; Cortesi, A.; Eva, F.; Elvassore, N. *Ind. Eng. Chem. Res.* **2003**, *42*, 3022.